How can satellite imagery be used to locate groundwater wells in semiarid region with crystalline basement?

Luís A. Magaia[*,**] and Katsuaki Koike[**]

*Faculty of Sciences, Eduardo Mondlane University, Ave. Mozambique km 1.5, P.O. Box 257, Maputo, Mozambique.
  E-mail: luisandremagaia@gmail.com
**Graduate School of Engineering, Kyoto University, Katsura C1-2-225, Kyoto 615-8540, Japan.

1. Introduction

In crystalline basement areas of the arid and semiarid regions, exploring for groundwater resources is challenging due to limited precipitation amount and high rates of evapotranspiration combined with the complex structurally controlled hydrogeology. Effective explorations in such areas have been achieved by geophysical surveys to locate thick zones of weathered basement. Such explorations require a considerable number of data, resulting in high cost of exploration, usually not affordable for many African countries.

In contrast, use of satellite imagery for groundwater survey has the advantage of providing spatially distributed measurements on a temporal basis over large areas, including areas inaccessible and insufficient in the coverage of detailed hydrogeological data. Another advantage is the availability of high resolution data supplied at no cost for research purposes.

This paper introduces a method that integrates optical and microwave sensor satellite images to support the drilling programs for water supply in crystalline basement rocks of arid and semiarid regions with less detailed hydrogeological data.

2. Study Area

The selected area is chiefly siting on the Mesoproterozoic rocks of Nampula complex, mainly composed of leucocratic quartz-feldspar gneiss, hornblende-bearing granodioritic gneiss, and banded biotite gneiss and migmatite (Lächelt, 2004; Macey et al., 2006). With 2025 km^2, it covers west of the Nampula and east of the Murrupula districts, Mozambique. Like many other areas located in the crystalline basement rocks of the country, problems in locating suitable groundwater wells have been reported in this area. Poor groundwater amount and quality are generally found in the zones of shallow weathered basement.

3. Data and Methodology

Two scenes representing the dry season: one from Sentinel-2A level 1C and another from the Advanced Land Observing Satellite (ALOS) Phased Array type L-band Synthetic Aperture Radar (PALSAR), and Digital Elevation Model (DEM) data from the Shuttle Radar Topographic Mission (SRTM) were selected for this study.

3.1 Linear Features

Fractures represent zones of rock weakness that can facilitate the groundwater flows and enhance the weathering of the subsurface rocks. In this study, extraction of lineaments, which are regarded as fracture-related topographic features, was performed using a non-filtering technique, Segment Tracing Algorithm, combined with a technique termed adaptive-tilt multi-direction shading (Masoud and Koike, 2011) using the DEM data.

3.2 Vegetation Index

Vivid vegetation in arid and semiarid regions during the dry season indicates richness of shallow groundwater zones. To access such zones, a vegetation index suitable for areas with sparse vegetation, a Modified Soil Adjusted Vegetation Index (MSAVI: Qi et al., 1994), was applied as:

$$\text{MSAVI} = \frac{2\rho_{b8} + 1 - \sqrt{(2\rho_{b8} + 1)^2 - 8(\rho_{b8} - \rho_{b4})}}{2} \qquad (1)$$

where ρ_{b4} and ρ_{b8} are the red and near infrared band reflectances, respectively.

3.3 Clay Index

Advance of weathering of the basement rocks induces development of secondary clay minerals such as kaolinite. Accessing such zones is implemented with a Modified Clay Index (MCI), in which a simple shortwave infrared (SWIR) band ratio ($\rho_{\text{SWIR1}}/\rho_{\text{SWIR2}}$) (Segal and Merin, 1989) is normalized by a simple vegation index ($\rho_{\text{NIR}}/\rho_{\text{Red}}$) (Jordan, 1969) as:

$$\text{MCI} = \frac{\rho_{\text{SWIR1}}/\rho_{\text{SWIR2}}}{\rho_{\text{NIR}}/\rho_{\text{Red}}} = \frac{\rho_{b11} \cdot \rho_{b4}}{\rho_{b12} \cdot \rho_{b8}} \qquad (2)$$

where ρ_{b11} and ρ_{b12} are the reflectances in the SWIR1 and SWIR2, respectively.

3.4 Surface Backscattering Coefficient

Abundance of clay minerals results in generation of smooth Earth surface. To convert the digital number of the microwave amplitude (DN) of the ALOS PALSAR image into surface backscattering coefficient (σ^0), an equation by Shimada et al. (2009) is applied as:

$$\sigma^0 = 10 \cdot \log_{10}(DN)^2 + K \qquad (3)$$

where K is the calibration factor.

4. Results and Discussion

The results of the study are summarized in maps of Figure 1. In the maps, the lineaments are distributed along narrows zones of high vegetation activity. Such

activity is also denounced by large σ^0 as the result of volumetric scattering due to vegetation. These zones are regarded to indicate shallow groundwater occurrence (Magaia *et al.*, 2018). The mountain area in the southeast is marked by poor clay content class and large σ^0 class. Despite showing active vegetation, its groundwater amount is probably small as the result of poor weathering of the granites due to slopping conditions that accelerate the runoff of precipitation. The north areas, dominated by small σ^0 and rich in clay content are regarded as areas of thick weathered regolith.

Moderate to active vegetation is also noticeable in these areas. High amount of groundwater is likely to be found in such zones if high lineament density occurs as similar to dense fault zones, because they promote weathering of the subsurface rocks. Conversely, the occurrence of dykes and sealed faults may pose barriers to groundwater movement. Our next step will consider the integration of subsurface structure obtained from geophysical explorations.

5. Concluding Remarks

This study represents preliminary results to access high groundwater potential zones in semiarid regions by an integration of optical and microwave data from satellite imagery. Zones along the lineaments in low land areas were regarded to indicate shallow groundwater occurrence. Clay-rich areas with low backscattered coefficient values were considered as occurrence of thick regolith in which large amount of groundwater is likely to be stored. Further integration of groundwater wells data and hydrogeological and geophysical data is expected to improve the present results and pinpoint with high accuracy potential zones to locate correctly groundwater wells in arid and semiarid regions.
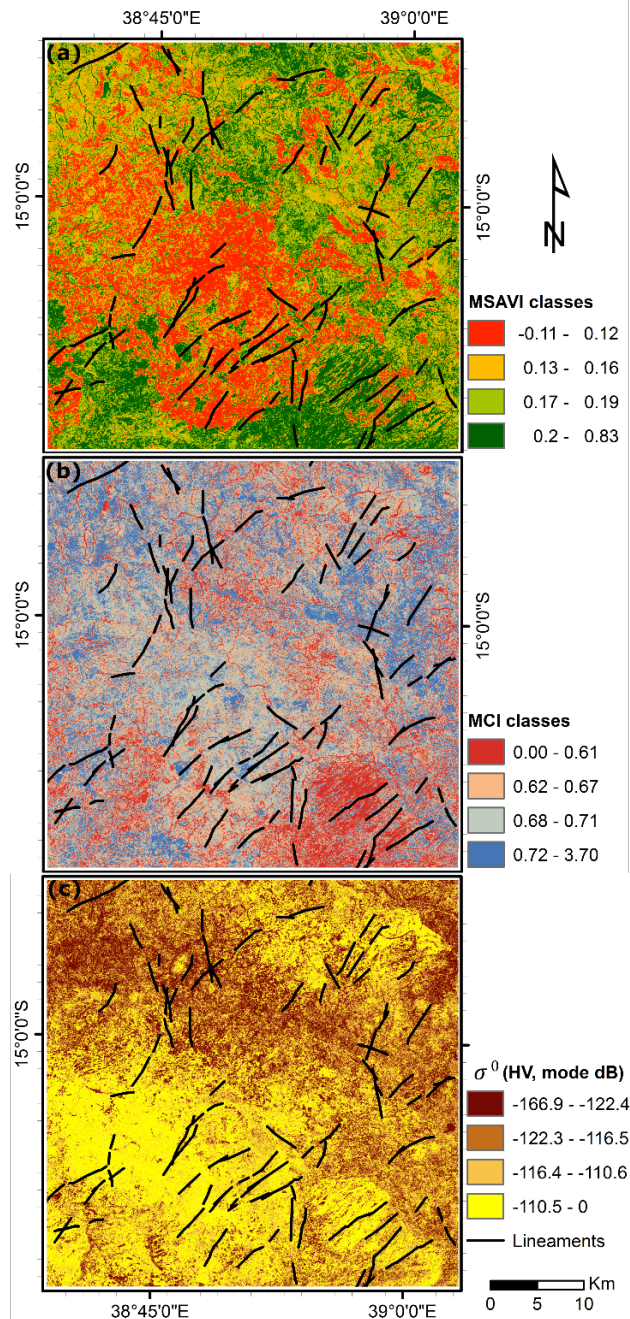

Fig. 1. Maps of the study area classified into four classes by quartiles of the following three parameter values distribution and overlain upon the lineaments: **(a)** Modified Soil Adjusted Vegetation Index (MSAVI) map in which red class is bare soil and vegetation activity increases from orange to dark green classes, **(b)** Modified Clay Index (MCI) map in which clay richness increases from red (poorest) to dark blue (richest) classes, and **(c)** surface backscattering coefficient map with the increase of surface roughness from dark brown to yellow classes.

References

Jordan, C. F. (1969) Derivation of Leaf-Area Index from quality of light on the forest floor. *Ecology*, 50(4), 663–666. doi:10.2307/1936256

Lächelt, S. (2004) *Geology and mineral resources of Mozambique*. Maputo: Ministério dos Recursos Minerais e Energia, Direcção Nacional de Geologia.

Macey, P., Ingram, B. A., Cronwright, M. S., Botha, G. A., Roberts, M. R., Grantham, G. H., et al. (2006) *Map explanation: sheets 1537, 1538, 1539, 1540, 1637, 1638 and 1630-40 scale 1:250,000*. Council of Geoscience, Pretoria, South Africa. Pretoria, South Africa: Council of Geoscience.

Magaia, L. A., Goto, T., Masoud, A. A., & Koike, K. (2018) Identifying groundwater potential in crystalline basement rocks using remote sensing and electromagnetic sounding techniques in central Western Mozambique. *Natural Resources Research*, 27(3), 275–298. doi:10.1007/s11053-017-9360-5

Masoud, A. A., & Koike, K. (2011) Auto-detection and integration of tectonically significant lineaments from SRTM DEM and remotely-sensed geophysical data. *ISPRS Journal of Photogrammetry and Remote Sensing*, 66(6), 818–832. doi:10.1016/j.isprsjprs.2011.08.003

Qi, J., Chehbouni, A., Huete, A. R., Kerr, Y. H., & Sorooshian, S. (1994) A modified soil adjusted vegetation index. *Remote Sensing of Environment*, 48(2), 119–126. doi:10.1016/0034-4257(94)90134-1

Segal, D. B., & Merin, I. S. (1989) Successful use of Landsat Thematic Mapper data for mapping hydrocarbon microseepage-induced mineralogic alteration, Lisbon Valley, Utah. *Photogrammetric Engineering and Remote Sensing*, 55(8), 1137–1145.

Shimada, M., Isoguchi, O., Tadono, T., & Isono, K. (2009) PALSAR radiometric and geometric calibration. *IEEE Transactions on Geoscience and Remote Sensing*, 47(12), 3915–3932. doi:10.1109/TGRS.2009.2023909